Journal of Physics: Conference Series **97** (2008) 012237 doi:10.1088/1742-6596/97/1/012237

Bulk nanocrystalline superconducting $YBa_2Cu_3O_{7-x}$

Jian Yong Xiang, Catherine Fleck, Damian P. Hampshire

Superconductivity Group, Department of Physics, Durham University, Durham DH1 3LE, United Kingdom

d.p.hampshire@durham.ac.uk

Abstract. A method to fabricate high density nanocrystalline superconducting $YBa_2Cu_3O_{7-x}$(YBCO) is presented in which commercially available YBCO powder is ball milled and then hot isostatically pressed (HIP'ed) at 0.2 GPa and 400 C. Ball milling decreased the average particle size from 2 μm to ~ 20 nm within 2 hours and to ~ 4 nm after milling for 30 hours with no noticeable strain. Ball milling increases the oxygen sublattice disorder and the Y/Ba anti-site disorder and drives the orthorhombic YBCO phase towards a disordered metastable cubic phase $Y_{1/3}Ba_{2/3}CuO_{3-x}$ consistent with the work by Simoneau *et al*. [14, 19]. Powders milled for 30 hours were HIPed at temperatures from 400 C to 550 C. At 450 C and above, the powder decomposed into the parent oxides. At 400 C, the metastable cubic phase reordered to form bulk YBCO with an average grain size of 5 - 18 nm and a relative mass density of ~ 96 %. The bulk YBCO material has an onset melting temperature and associated enthalpy of 970 ^oC and 157 $J.g^{-1}$ respectively which can be compared to 965 ^oC and 156 $J.g^{-1}$ for the starting commercial powder. These results are consistent with XRD data and they suggest a predominantly single-phase nanocrystalline YBCO has been fabricated. The superconducting transition temperature (T_C) of the nanocrystalline YBCO determined from ac. susceptibility measurements is 88.8 K, with a slope of upper critical field near T_C of ~ 0.12 $T.K^{-1}$.

1. Introduction

Conventional ceramic fabrications techniques for $YBa_2Cu_3O_{7-x}$ (YBCO) result in low superconducting critical current density (J_C). This is attributed to weak transmission across d-wave grain boundaries at large misorientation angles [1-5]. Several techniques have been investigated to increase J_C, including increasing the flux pinning through nano-particle additions [6] and improving the superconducting properties of the grain boundary [7-9]. Unfortunately pinning effects that come from the nanoscale disorder in the materials are drastically weakened by a large anisotropy in YBCO [10], and it is not clear that pinning within the grains will increase the macroscopic J_C. However, improving the grain boundaries has led to significant improvements. Second generation $YBa_2Cu_3O_{7-x}$ (YBCO) coated conductors consist of highly aligned quasi-single-crystalline coated conductors and carry high J_C. They have the performance needed for power transmission cables, but the ac. losses remain quite high for rotating machinery and transformer applications because of the planar, rather than multifilamentary, geometry of the coated superconductor.

In this paper, we describe fabrication of bulk nanocrystalline YBCO using ball milling and Hot Isostatic Pressing (HIP). If polycrystalline material can be fabricated with high J_C, one can expect the improvements in powder-in-tube processing made over the last decade to lead to low ac. loss

filamentary conductors made with YBCO. A number of improvements are possible in high density nanocrystalline YBCO materials: Flux pinning is expected to be very strong in high density, nanocrystalline samples prepared by ball milling [11-13]; The grain boundaries may be very clean due to the improved diffusion under high pressure; The densification of the material can improve the connectivity between grains thereby increasing J_C [15, 16], and the upper critical field (B_{C2}) in the nano-structured superconductors may be increased by shortening the electron mean-free-path as has been found in the conventional superconductors such as Chevrel phase [11], elemental [17] and A15 compounds [18]. Improving B_{C2} of YBCO is particularly important for high magnetic field applications operating at liquid nitrogen temperatures.

Fabrication of nanocrystalline YBCO powder has been reported previously [14, 19-21] with limited measurements in high magnetic fields. This work describes how to use ball milling and hot isostatic pressing to fabricate bulk high density nanocrystalline YBCO. X-ray diffraction (XRD) and thermal analysis measurements are used to characterise the structural properties. Ac. susceptibility measurements characterise some of the properties in magnetic fields up to 9 T.

2. Preparation and properties of milled nanocrystalline powder

Powders of commercial $YBa_2Cu_3O_{7-x}$ (99.9%, Goodfellow), with an initial average grain size ~ 2.8 μm, were used as the starting materials. A planetary miller (Fritsch Pulverisette 6) was used with air cooling. A copper pot and ten copper balls with different diameters (three 20 mm and seven 10 mm diameter balls) were used to grind the powder. Copper was used since copper has less of an adverse effect on the superconductivity of YBCO than other (harder) milling media such as Nb, hard steel and tungsten carbide. The ball to powder mass ratio was 10:1 and 15 g of YBCO powder was placed into the pot in air. A rotating speed of 300 rpm was used and the milling was paused for 5 minutes every half hour to prevent excess heating of the sample and overheating of the miller. The pot was scraped regularly during the milling cycle with a copper rod to increase the yield. The final product was milled for 30 hours and had a yield of ~ 85 % of the initial powder. The powder was taken out of

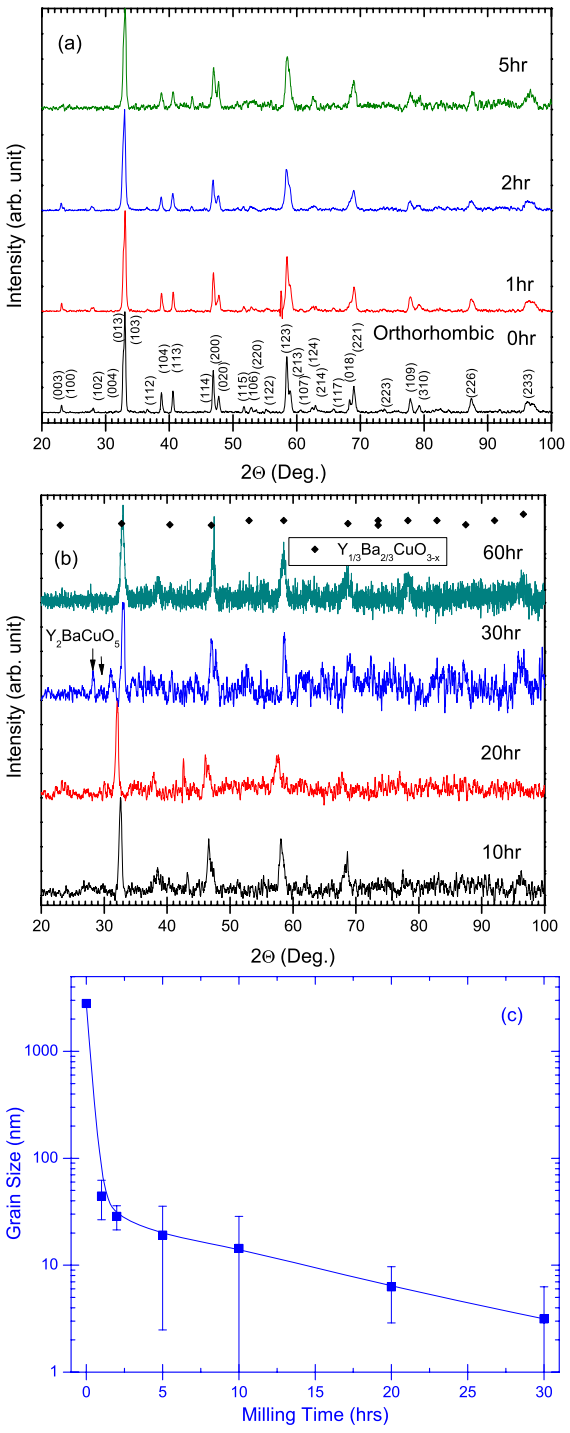

Figure 1: X-ray diffraction patterns of YBCO after different milling time (a) 0-5 hours and (b) 10-60 hours. (c) Average particle size versus milling time. Solid symbols are the theoretical peaks for cubic $Y_{1/3}Ba_{2/3}CuO_{3-x}$ [14]. The background has been fitted and subtracted from the data.

the pot regularly to monitor the structure using XRD (Siemens d5000). Figure 1(a) and 1(b) show the XRD patterns of the YBCO powder milled for different times. The starting material was orthorhombic. For the milling times longer than 5 hours, the orthorhombic peaks broaden and become tetragonal.

Simoneau *et al.* [23] have shown that a short period of mechanical milling primarily affects the oxygen sublattice but produces little change in the oxygen content. After 5 hours of milling, the oxygen disorder is associated with a transition from an orthorhombic to a high oxygen content disordered tetragonal structure. At 30 hours milling, the site anti-site disorder in the Y and Ba cations and strain from the deformed oxygen lattice tends to drive the tetragonal phase towards a cubic metastable structure $Y_{1/3}Ba_{2/3}CuO_{3-x}$ [20, 19, 21] as shown by the solid square symbols in figure 1(b). The presence of Y_2BaCuO_5 is due to the water contamination of YBCO [22]. No further changes in the diffraction pattern occurred between 30 hours and 60 hours. The average particle size and strain in the different stages of milling were estimated from XRD data using the commercial software programme TOPAS. Figure 1(c) shows that the grain size decreased markedly in the first two hours of milling from ~ 2.8 μm to ~ 20 nm, but the strain was almost unaffected. Thereafter changes in grain size with increased milling time were relatively small. Powders milled for 30 hours had a grain size of ~ 4 nm.

High temperature thermogravity analysis (TGA) and differential scanning calorimetry (DSC) were performed simultaneously using an STA, Netzsch Jupiter 499C which includes a high accuracy specific heat capacity (c_P) sample carrier. Alumina pans and lids were used and conditioned under vacuum prior to use. Flowing argon was used as the protective gas. The instrument was calibrated by measuring the melting points of standard samples including tin, aluminum, zinc, bismuth and gold and measuring c_P for a 0.75 mm thick sapphire plate. Typically ~ 50 mg of sample was measured at a heating rate of 20 $K.min^{-1}$. Figure 2 shows c_P (defined as the heat capacity divided by the instantaneous mass of the sample) and the mass change as a function of temperature for the powder milled for different times. Figures 2(a) and 2(b) show the properties of the starting commercial material (unmilled) and the milled

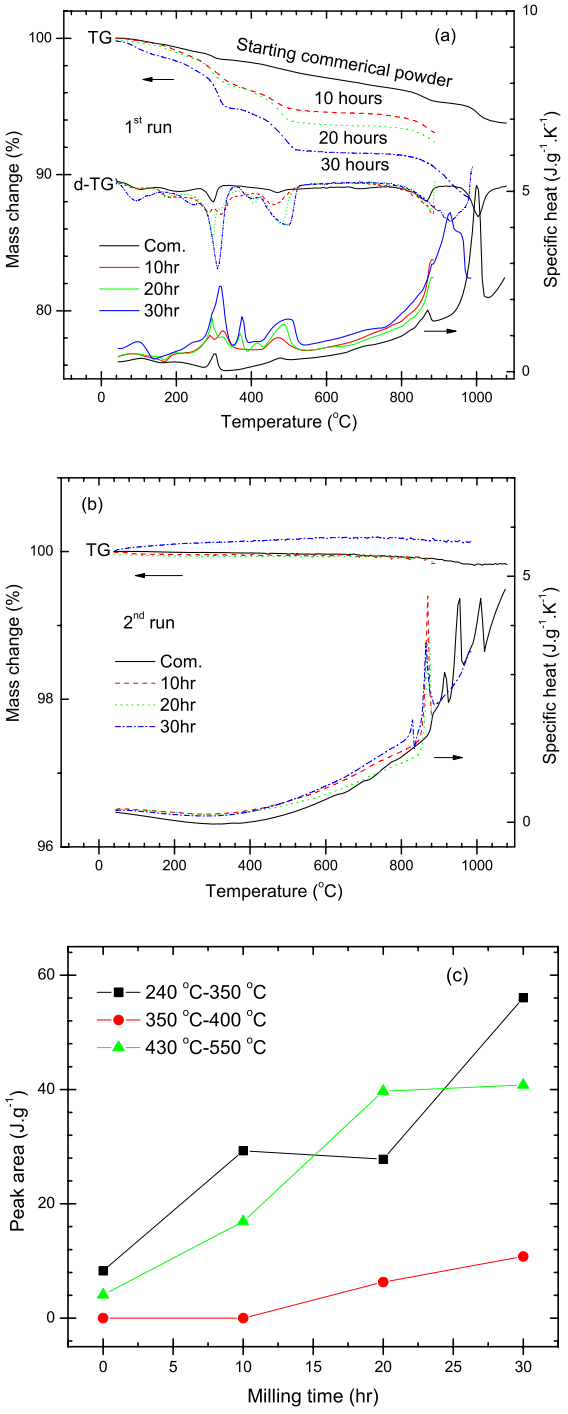

Figure 2: Thermogravity and specific heat as a function of temperature for the powders milled in different temperatures. (a) and (b) is the 1st run and 2nd run results, respectively. Derivative of the thermogravity (d-TG) is present in (a) as well. (c) is the peaks area of the specific heat changes with milling time.

powders, which were measured during the first heating cycle (1st run) and during the second heating cycle (2nd run). Comparing the two runs allows us to distinguish melting (where peaks occur in both runs) from microstructural and decompositional changes (that only occur in the first run).

Mass loss at temperatures below 140 ^{o}C is associated with the removal of moisture and decomposition of hydrates since the powders were handled in air [22, 23]. The reduction in mass for the unmilled commercial powder between 400 ^{o}C and 800 ^{o}C is ~ 2.3 %, which corresponds to the oxygen loss of YBCO from O_7 to O_6. Powders milled for 30 hours looks moist, consistent with milled fine powder reacting with moisture (and carbon dioxide). There are three main peaks in the c_P data in the ranges 250 ^{o}C - 350 ^{o}C, 350 ^{o}C - 400 ^{o}C and 430 ^{o}C - 550 ^{o}C. The peak at 240 ^{o}C - 350 ^{o}C can be attributed to the decomposition of $Ba(OH)_2$ due to the exposure of the powder to air. The peak in the range from 350 ^{o}C - 400 ^{o}C is structural since there is no change of mass. We suggest this is a crystallographic transformation from the metastable cubic structure back to the YBCO structure [14]. Consistent with this interpretation, the equivalent peak is not observed in the unmilled sample. At the temperatures of the highest peak between 450 ^{o}C and 600 ^{o}C, following the previous work [14, 20], we suggest the cubic phase decomposes into a combination of 123, parent oxides and oxygen where $9\ Y_{1/3}Ba_{2/3}CuO_{3-x} \rightarrow YBa_2Cu_3O_{7-y} + Y_2BaCuO_5 + 1.5\ Ba_2Cu_3O_{5.9} + 0.5\ CuO + (2.825\text{-}4.5x+0.5y)\ O_2$, and at about 540 ^{o}C in air $Ba_2Cu_3O_{5.9}$ further decomposes through $Ba_2Cu_3O_{5+x} \rightarrow 2\ BaCuO_2+CuO+ 0.5x\ O_2$ [24]. The areas of the three c_P peaks are plotted as a function of the milling time in figure 2(c). The areas of these peaks increase with milling time and disappear during the 2nd run as expected. Peaks in c_P at temperatures above 850 ^{o}C are associated with melting and with further decomposition and reduction in mass. Early studies[25] have shown that the melting point of YBCO is dependent on the oxygen content dependent at around 950 ^{o}C - 980 ^{o}C in an argon atmosphere and at higher temperature in air [26]. The peak with an onset ~ 860 ^{o}C can be associated with $BaCu_2O_2$ melting which is only stable at a very low oxygen partial pressure [24] and the peak at 1100 ^{o}C in the unmilled powder is probably the decomposition of YBCO.

3. Fabricating HIPed materials

The powder milled for 30 hours was stored in a glove box (< 10 ppm water) for one month. It was then wrapped in Nb foil, which served as a diffusion barrier, and subsequently sealed under vacuum in stainless steel. Hot isostatic pressing was performed at 2000 bar for 5 hours at different temperatures. After HIP'ing, samples were extracted, polished to remove the barrier layer, and cut into regular shapes for the magnetic measurements.

About 100 mg of the HIP'ed sample was ground for the XRD measurements. Figure 3(a) shows the XRD data for the powder that was milled for 30 hours and subsequently HIP'ed at different temperatures. At HIP'ing temperatures of 450 ^{o}C and above, parent oxide phases such as YOOH, $BaCO_3$, CuO, $Ba(OH)_2(H_2O)_3$ and Y_2O_3 are found. The average grain size for the 400 ^{o}C HIP'ed sample was estimated to be ~ 5 nm which is close to the size of the milled powder before the HIP treatment. The XRD data is predominantly broadened YBCO Bragg peaks. The commercial powder was also HIP'ed as a control and XRD data are presented in figure 3(b). The predominant phase is YBCO within which the oxygen content decreased as the HIP'ing temperature increased. The commercial powder HIP'ed at 750 ^{o}C shows a tetragonal structure with the oxygen content estimated from XRD to be ~ 6.32. A small amount of Y_2BaCuO_5 is also present. A relative mass density of 96 ± 4% was estimated by measuring a carefully polished rectangular bar of the sample. Specific heat and TG were used to characterize the HIPed samples. The milled powders were HIP'ed at 400 ^{o}C (denoted M400), part of which was subsequently annealed in oxygen 750 ^{o}C (denoted M400A), and HIP'ed at 450 ^{o}C (denoted M450). The unmilled samples were starting commercial powder HIP'ed at 400 ^{o}C (denoted U400), part of which again was oxygen annealed at 750 ^{o}C (denoted U400A), and HIP'ed at 550 ^{o}C (denoted U550). Figures 4(a) and 4(b) show the specific heat and TG for the HIP'ed samples for the first and second heating run respectively. The first run for M450 has many peaks consistent with the decomposition shown by the XRD data. For M400, U400 and the commercial powder, the peaks in the specific heat data and mass change are similar. The onset and area of the large peak

around 1000 °C for M400, U400 and the commercial powder are (970 °C, 157.1 J.g^{-1}), (961 °C, 139.9 J.g^{-1}) and (965 °C, 156.4 J.g^{-1}), respectively. Theoretical calculations show the enthalpy associated with melting $YBCO_7$ and $YBCO_6$ in air are 235.4 J.g^{-1} and 258.7 J.g^{-1} respectively [27]. This is higher than observed here partly because we have used an Argon atmosphere. We associate the peaks for U400, M400 and the commercial powder around 965 °C with the melting of YBCO, and given the similarities in enthalpy (and the similarities in XRD), interpret these data as evidence that M400 is predominantly single-phase nanocrystalline YBCO. No peaks are seen below 800 °C for the second run.

4. Measurements of superconducting properties

Ac. susceptibility measurements were carried out using a physical properties measurement system (PPMS, Quantum Design) in magnetic fields up to 9 Tesla. An ac. magnetic field with a 4 Oe amplitude and 777 Hz was used to measure the real part of the ac. susceptibility. Data for the M400 sample as a function of temperature and magnetic field are shown in figure 5. The transition is quite broad as expected for nanocrystalline material. Table 1 shows the superconducting transition (T_C),

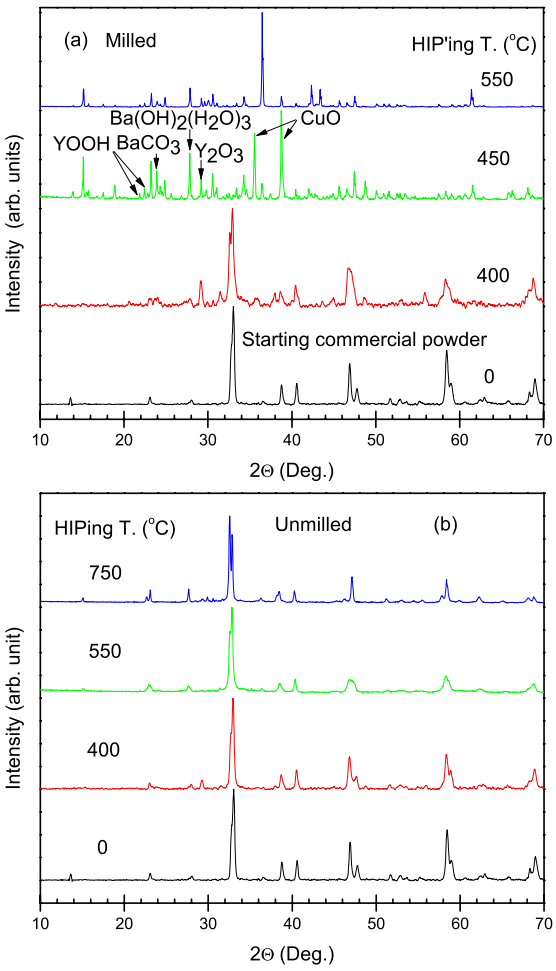

Figure 3: (a)XRD patterns of YBCO after HIPing. (a) Powder milled for 30 hours and HIP'ed at different temperatures. (b) Unmilled powder HIP'ed at different temperatures. The XRD pattern of the starting commercial YBCO powder is shown for comparisons.

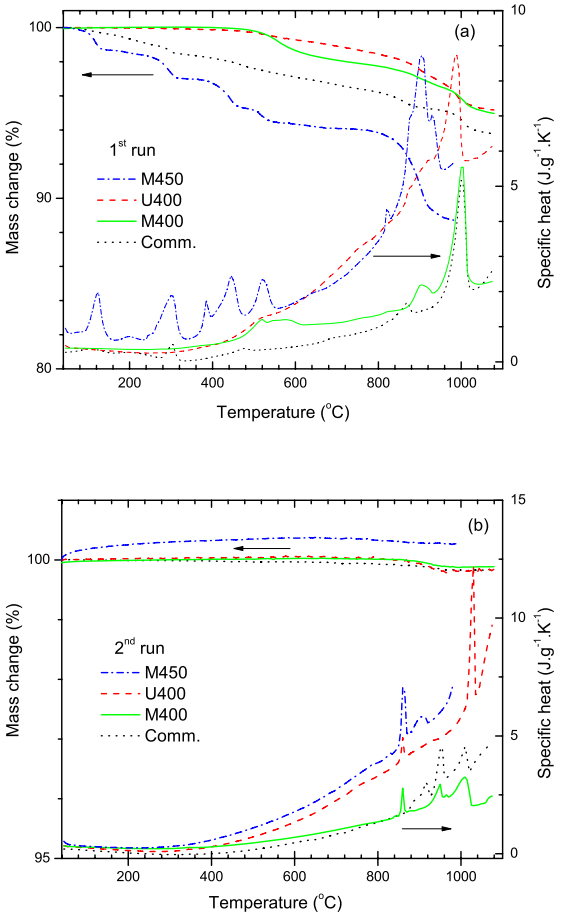

Figure 4: Specific heat and TG of HIP'ed samples HIP'ed (a) the 1st run and (b) 2nd run. These samples include milled and HIPed at 400 °C (M400) and 450 °C (M450), unmilled and HIP'ed at 400 °C (U400) and commercial starting powder (comm.).

Table 1: The T_C dependence of the slope of upper critical field dB_{C2}/dT near T_C for HIP'ed YBCO (milled and unmilled), commercial powder and a single crystal.

Sample	Unmilled commercial power	Unmilled commercial powder (U) and milled powder (M) subsequently HIP'ed at different temperatures and oxygen annealed (A)						YBCO Single crystal	
		U550	U400	U400A	M400	M400A	M450	//c-axis	⊥c-axis
T_C (K)	92.0	52.4	83.6	91.8	88.8	91.9	< 3	90.7	
dB_{C2}/dT ($T.K^{-1}$)	0.297	0.06	0.112	0.179	0.124	0.209	-	0.282	1.369

which was determined from the onset of magnet shielding, for milled (M) and unmilled (U) HIPed samples. T_C decreases with increased HIP'ing temperature for the unmilled samples due to the loss of oxygen starting from ~ 400 °C and is consistent with the XRD results. T_C for samples HIPed at 400 °C is 83.6 K and 88.8 K for unmilled and milled samples respectively. Oxygen annealing increased T_C of U400 and M400 by ~ 8 K and ~ 3 K to 91.8 and 91.9 K, respectively. This indicates nearly optimal oxygen content in the M400 sample. Furthermore, an increase of the diamagnetic signal was observed for M400 after oxygen annealing which was probably due to grain growth. For the M450 sample, no superconductivity was found down to 3K which is consistent with the XRD data. T_C measured in different magnetic fields for the milled samples are presented in figure 6. For comparison, results of the commercial powder and single crystals are also presented. At 400 °C, B_{C2} of milled samples are higher than equivalent unmilled samples which may be due to the higher oxygen content. Oxygen annealing after HIP'ing improved B_{C2} and reduced the difference between milled and unmilled samples. The slopes of B_{C2}(T) with respect to temperature in table 1 were obtained by fitting the data points between 0.25 and 1 T and is about one half of the slope for the single crystal in the *c*-direction.

5. Discussions and conclusion

The samples produced by HIP'ing at 400 °C are clearly different from the multiphase samples produced by milling and sintering at ambient pressure. By HIP'ing at 400 °C and 0.2 GPa, one can avoid the decomposition of the metastable cubic phase $Y_{1/3}Ba_{2/3}CuO_{3-x}$ into parent oxides. The low

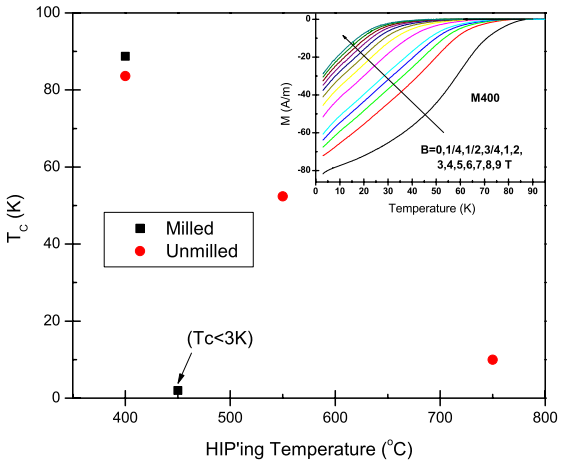

Figure 5: Superconducting transition temperature varies with the HIP'ing temperature for the HIP'ed samples. T_C was determined from the onset point of the real part of the ac. susceptibility. Inset shows the ac. susceptibility of the sample milled and HIP'ed at 400 °C measured from 3 K – 95 K.

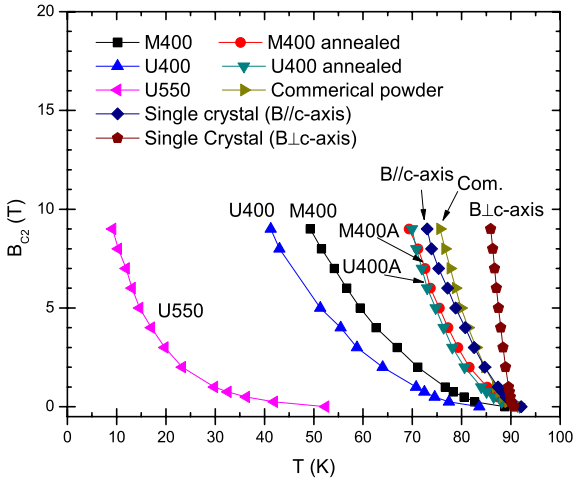

Figure 6: Upper critical fields of the HIP'ed samples. B_{C2} were determined from the real part of the ac. susceptibility. Data of commercial powder and single crystal are presented as well for a comparison.

HIP temperature helps to keep the oxygen in the sample and minimizes the chemical reactions which lead to decomposition and redundant phases. High density superconducting nanocrystalline YBCO has been successfully fabricated at 400 ^{o}C. The nanocrystalline sample has a T_C of ~89 K and a slope of B_{C2}(T) near T_C of 0.12 T.K^{-1}. T_C was marginally increased by oxygen annealing at 750 ^{o}C after the HIP processing which can be attributed to the growth of grain. Further work is required to investigate the properties of high quality single phase superconducting nanocrystalline YBCO.

Acknowledgments
The authors would like to thank Prof. John Evans for help with the XRD measurements, and Dr. Joshua Higgins for useful discussions. This work is funded by EPSRC and NEDO (Applied Superconductivity).

References

[1] Ayache J 2006 *Philos. Mag.* **86** 2193
[2] Dimos D, Chaudhari P and Mannhart J 1990 *Phys. Rev. B* **41** 4038
[3] Dimos D, Chaudhari P, Mannhart J, *et al.* 1988 *Phys. Rev. Lett.* **61** 219
[4] Gurevich A and Pashitskii E A 1998 *Phys. Rev. B* **57** 13878
[5] Hilgenkamp H and Mannhart J 2002 *Rev. Mod. Phys.* **74** 485
[6] Haugan T, Barnes P N, Wheeler R, *et al.* 2004 *Nature* **430** 867
[7] Hammerl G, Schmehl A, Schultz R R, *et al.* 2000 *Nature* **407** 162
[8] Parikh A S, Meyer B and Salama K 1994 *Superconductor Science & Technology* **7** 455
[9] Ahn J H and Ha K H 1996 *Mat Sci For* **225 - 227** 923
[10] Blatter G, Feigelman M V, Geshkenbein V B, *et al.* 1994 *Rev. Mod. Phys.* **66** 1125
[11] Niu H J and Hampshire D P 2003 *Phys. Rev. Lett.* **91** 027002
[12] Niu H J and Hampshire D P 2004 *Phys. Rev. B* **69** 174503
[13] Gumbel A, Eckert J, Fuchs G, *et al.* 2002 *Appl. Phys. Lett.* **80** 2725
[14] Simoneau M, L'Esperamce G and Schulz R 1994 *J. Appl. Phys.* **76** 136
[15] Aslan M, Jaeger H, Schulze K, *et al.* 1990 *Journal of the American Ceramic Society* **73** 450
[16] Tomita T, Schilling J S, Chen L, *et al.* 2006 *Phys. Rev. B* **74**
[17] Bose S, Raychaudhuri P, Banerjee R, *et al.* 2006 *Phys. Rev. B* **74**
[18] Cooley L D, Hu Y F and Moodenbaugh A R 2006 *Appl. Phys. Lett.* **88**
[19] Lavallee F, Simoneau M, L'Esperance G, *et al.* 1991 *Phys. Rev. B* **44** 12003
[20] Fang H and Ravi-Chandar K 1998 *J. Supercond.* **11** 555
[21] Xu X L, Guo J D, Wang Y Z, *et al.* 2002 *Physica C-Superconductivity and Its Applications* **371** 129
[22] Yan M F, Barns R L, Obryan H M, *et al.* 1987 *Appl. Phys. Lett.* **51** 532
[23] Sargankova I, Diko P, Tweed J D, *et al.* 1996 *Superconductor Science & Technology* **9** 688
[24] Voronin G F and Degterov S A 1994 *J. Solid State Chem.* **110** 50
[25] Sestak J 1992 *Pure and Applied Chemistry* **64** 125
[26] Vajpei A and Upadhyaya G eds 1992 *Powder Processing of High Tc oxides Superconductors* (Switzerland: Trans Tech Publication Ltd)
[27] Sestak J, Moiseev G K and Tzagareishvili D S 1994 *Japanese Journal of Applied Physics Part 1-Regular Papers Short Notes & Review Papers* **33** 97